Electronic Supplementary Information (ESI)

Facile synthesis and enhanced sodium storage performance of chemically bonded CuP_2/C hybrid anode

Sang-Ok Kim and Arumugam Manthiram*

Materials Science and Engineering Program & Texas Materials Institute, The University of Texas at Austin, Austin, TX 78712, USA.

E-mail address: rmanth@mail.utexas.edu

Experimental Section

Synthesis: The CuP_2/C hybrid sample was synthesized by a simple one-step high energy mechanical milling (HEMM) method. Commercial red phosphorus (98+%, Alfa Aesar), copper (99%, 45 μm, Acros Organics), and acetylene black carbon (–200 mesh, Alfa Aesar) powders were used as raw materials for the synthesis without further treatment. Elemental red phosphorus and copper powders were mixed with a molar ratio of 2 : 1 and further blended with different amounts of acetylene black carbon (10, 20, and 30 wt. %). The mixture was placed in a hardened stainless steel vial (80 cm^3) with hardened steel balls and sealed in an argon-filled glovebox followed by HEMM at a rotation rate of 1060 rpm for 3 h at room temperature with a SPEX 8000M machine. The total mass of the powder was 2.0 g and a ball-to-powder weight ratio was fixed at 20 : 1. The obtained powder samples were stored in a vacuum desiccator in order to minimize surface oxidation. For a comparison, pure CuP_2 was also prepared without acetylene black carbon by the same procedure described above. Then, CuP_2 was simply mixed with 20 wt. % of carbon by hand grinding to obtain the CuP_2/C composite in order to check the effect of P–O–C bonding on the electrochemical

performance of the CuP_2/C hybrid.

Structural and morphological Characterizations: The structural characterizations of the samples were carried out with X-ray diffraction (XRD: Rigaku MiniFlex 600) with Cu Kα (λ = 1.54059 Å) radiation, X-ray photoelectron spectroscopy (XPS: Kratos Analytical), and Fourier transform infrared spectroscopy (FTIR: Thermo Scientific Nicolet iS5). Scanning electron microscopy (SEM: JEOL JSM–5610) with energy dispersive X-ray spectroscopy (EDS), scanning transmission electron microscopy (STEM: Hitachi S–5500), and transmission electron microscopy (TEM: JEOL 2010F) were used to analyze the surface morphology and elemental distribution of the powder samples. The carbon content was estimated by thermogravimetric analysis (TGA: Netzsch STA449 F3 Jupiter) and the tap density of the samples was determined with a Quantachrome AT–4 Autotap machine.

Electrochemical Measurements: The electrodes were fabricated by depositing slurries containing 70 wt. % active material, 15 wt. % conducting agent (Super P), and 15 wt. % poly(acrylic) acid (PAA) binder (MW ~250,000, 35 wt. % in water, Aldrich) onto a copper foil current collector, followed by drying in a vacuum oven at 120 ^{o}C for over 8 h. Then, the electrodes were cut into disks with an area of 1.13 cm^2. The typical loading mass of the active materials was ~ 2.0 mg cm^{-2}. The CR2032 coin cells were fabricated inside an argon-filled glove box by employing polypropylene (Celgard 2500) separator and sodium foil counter/reference electrode. The electrolyte used was 1.0 M $NaClO_4$ in a mixture of ethylene carbonate (EC) and diethyl carbonate (DEC) (1 : 1 v/v) with the addition of 5 vol. % of fluoroethylene carbonate (FEC) additive. Galvanostatic cycling tests were performed with a battery testing system (Arbin BT–2000) within a voltage range of 0.0 – 1.5 V (vs. Na / Na^+). Electrochemical impedance spectroscopy (EIS) experiments were carried out with an impedance/gain-phase analyzer (Solartron SI 1260A) combined with an electrochemical

interface (Solartron SI 1287A) with the ac amplitude of 5 mV over a frequency range from 100 kHz to 0.1 Hz. For the *ex-situ* XRD and SEM analyses, the electrodes were collected by disassembling the test cells in the argon-filled glove box, rinsing with DEC several times, and drying at room temperature.

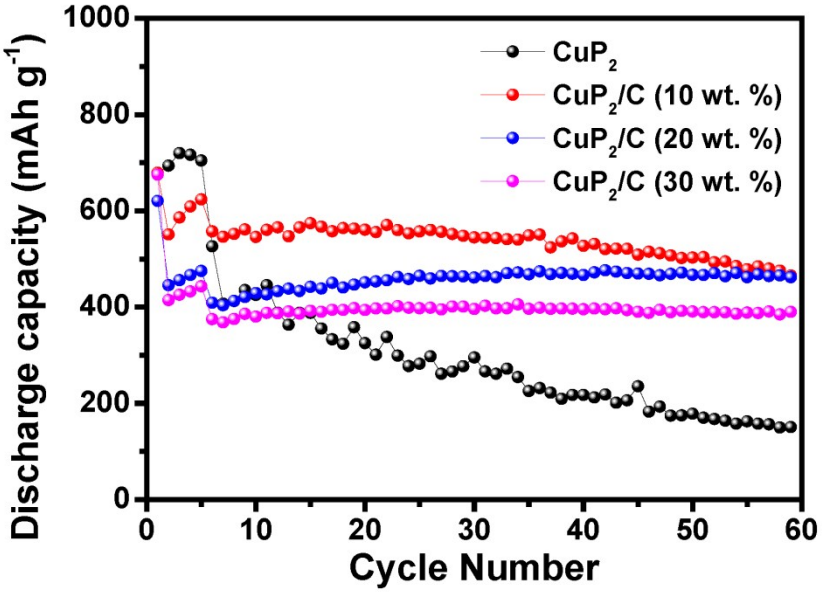

Figure S1. Cycle performance of pure CuP_2 and CuP_2/C hybrids with different amounts of carbon at a current density of 200 mA g^{-1} within a voltage range of 0.0 – 1.5 V (vs. Na / Na^+). The cells were tested at 50 mA g^{-1} for the initial 5 cycles for activation.

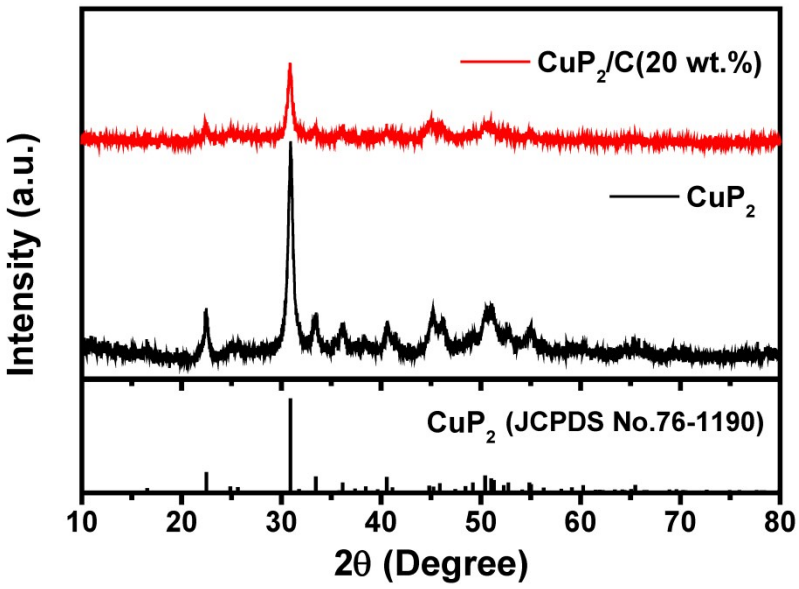

Figure S2. XRD patterns of pure CuP_2 and CuP_2/C hybrid synthesized by HEMM for 3 h.

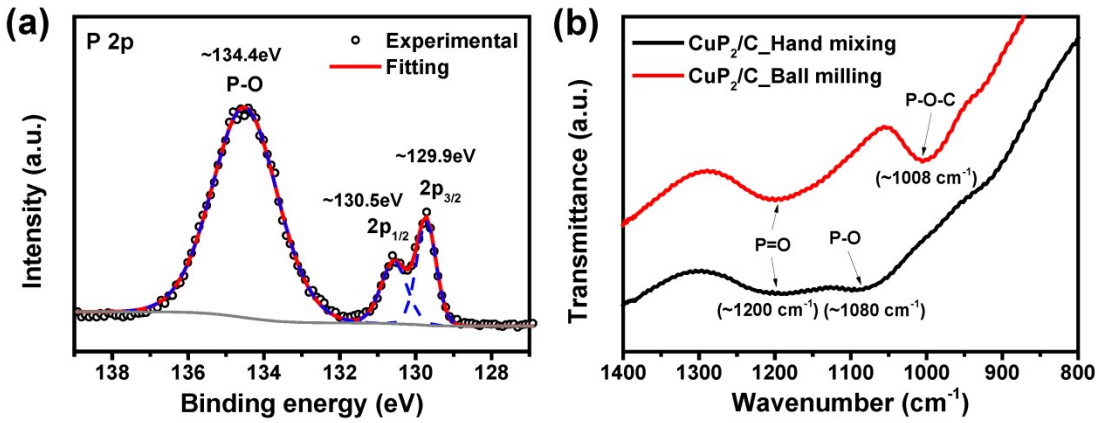

Figure S3. (a) XPS P 2p spectrum of elemental phosphorus. (b) Comparison of the FTIR spectra of the hand-mixed CuP_2/C (20 wt. % carbon) composite and ball-milled CuP_2/C (20 wt. % carbon) hybrid.

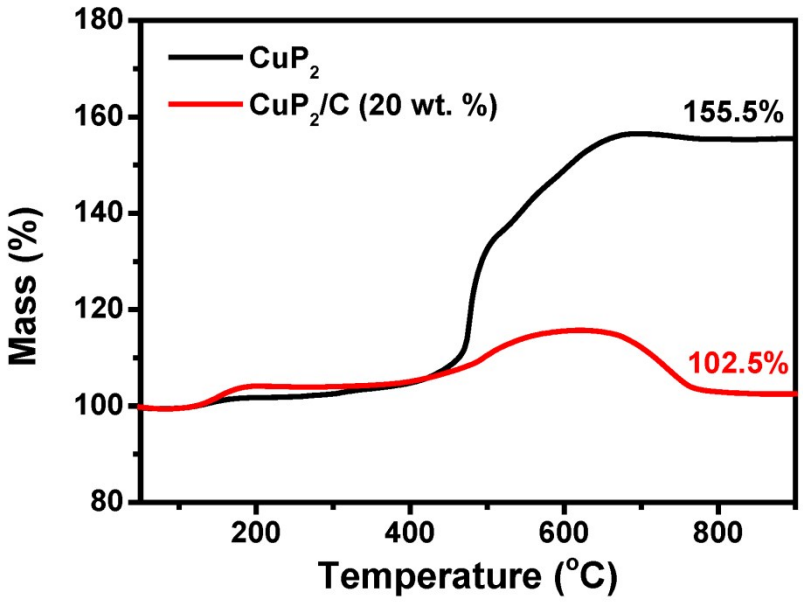

Figure S4. TGA curves of pure CuP_2 and the CuP_2/C (20 wt. % carbon) hybrid.

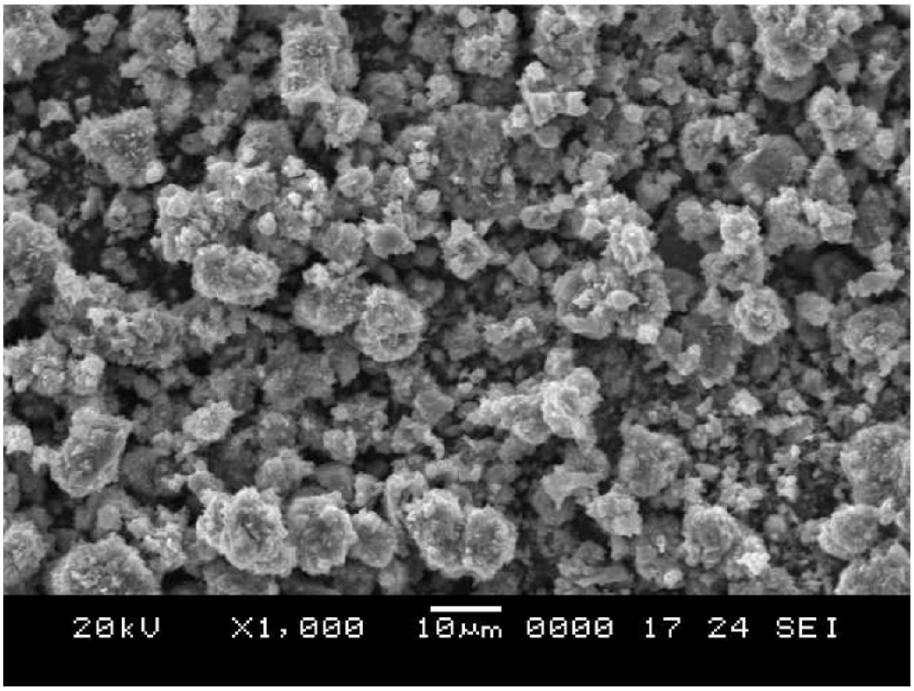

Figure S5. SEM image of pure CuP_2 synthesized by HEMM for 3 h.

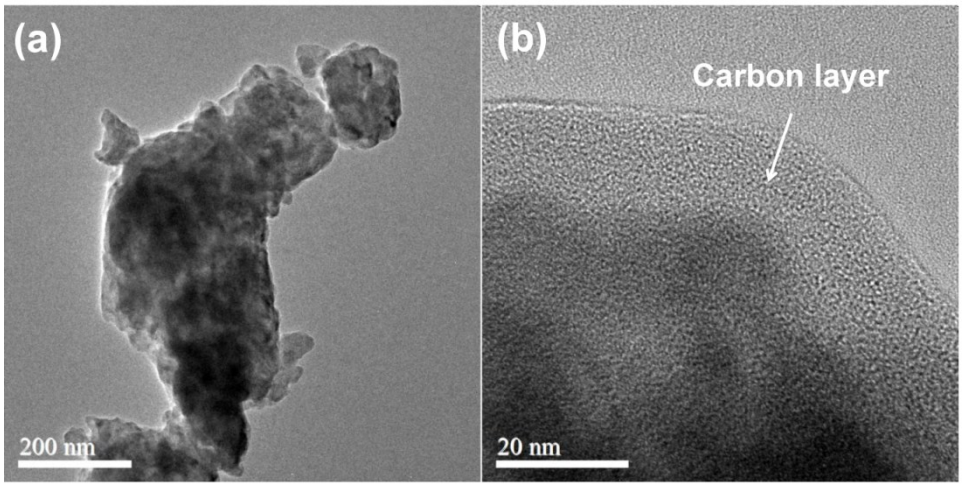

Figure S6. (a) Low- and (b) high-magnification TEM images of the CuP_2/C hybrid.

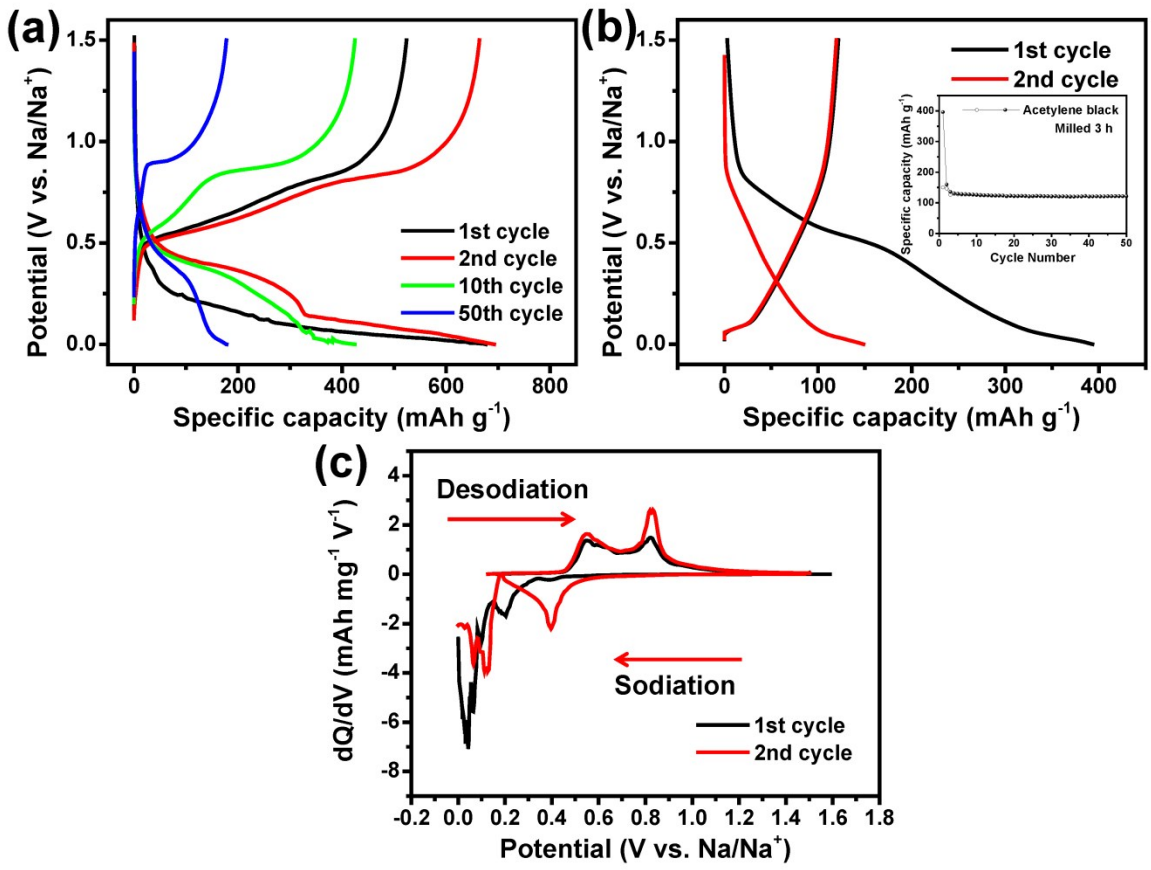

Figure S7. Voltage profiles of the (a) pure CuP_2 and (b) milled acetylene black electrodes at various cycle numbers. The inset in (b) shows the cycle performance of the milled acetylene black. (c) Differential capacity plots (DCPs) of the pure CuP_2 electrode at initial two cycles.

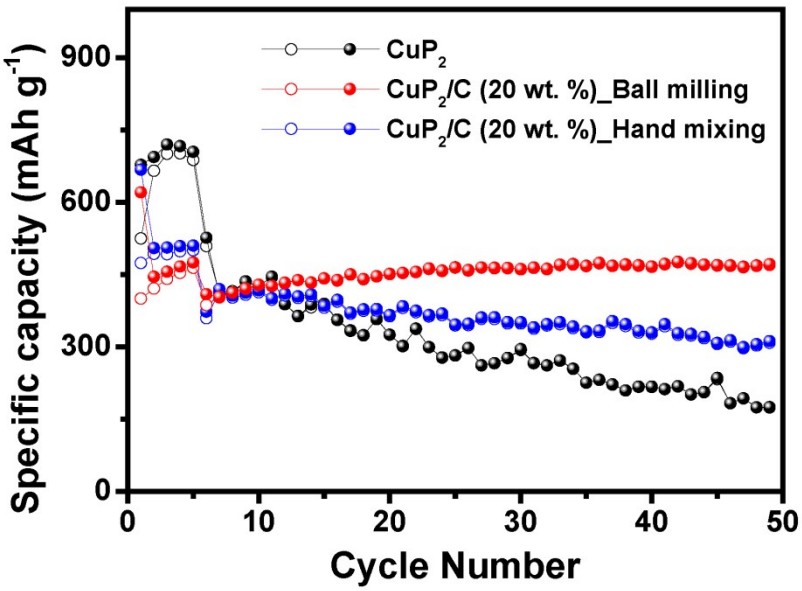

Figure S8. Comparison of the cycle performances of pure CuP_2, hand-mixed CuP_2/C composite, and ball-milled CuP_2/C hybrid electrodes at a current density of 200 mA g^{-1}. The cells were tested at 50 mA g^{-1} for the initial 5 cycles for activation.

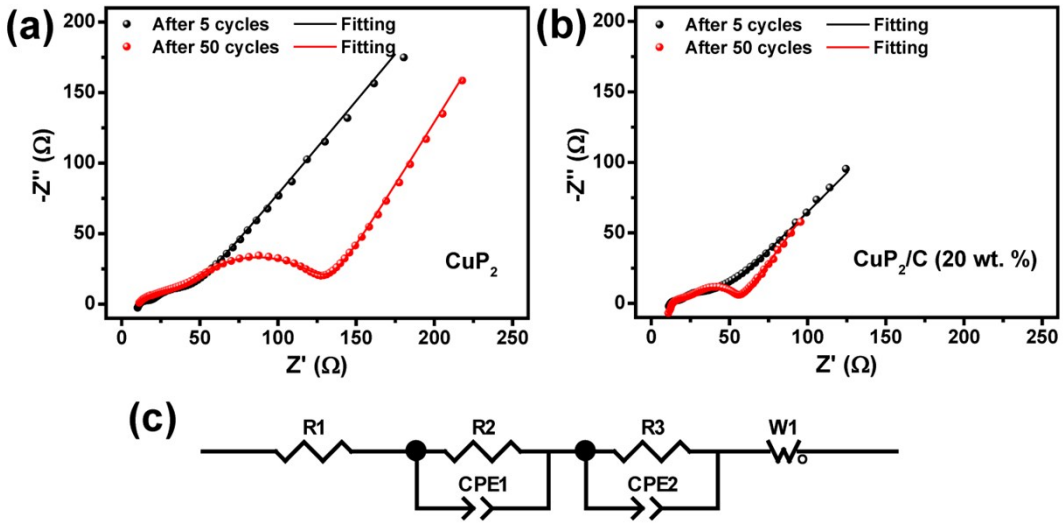

Figure S9. Impedance spectra and curve fitting results for the (a) pure CuP_2 and (b) CuP_2/C hybrid electrodes after 5 and 50 cycles. (c) Simplified equivalent circuit used for the curve fitting.

Variations of the resistance component values of the CuP_2 and CuP_2/C hybrid electrodes

Electrode	Component	Resistance (Ω)	
		at 5 cycles	at 50 cycles
CuP_2	R_s	11.8	9.9
	R_{int}	5.0	34.0
	R_{ct}	25.7	84.8
CuP_2/C (20 wt.%) hybrid	R_s	12.4	14.2
	R_{int}	3.0	6.8
	R_{ct}	29.1	35.3

Components of the simplified equivalent circuit:

R1(R_s): Electrolyte resistance, W1: Warburg impedance

R2 (R_{int}): Interfacial resistance, CPE1: Constant phase element of interface

R3 (R_{ct}): Charge-transfer resistance, CPE2: Constant phase element of charge-transfer reaction

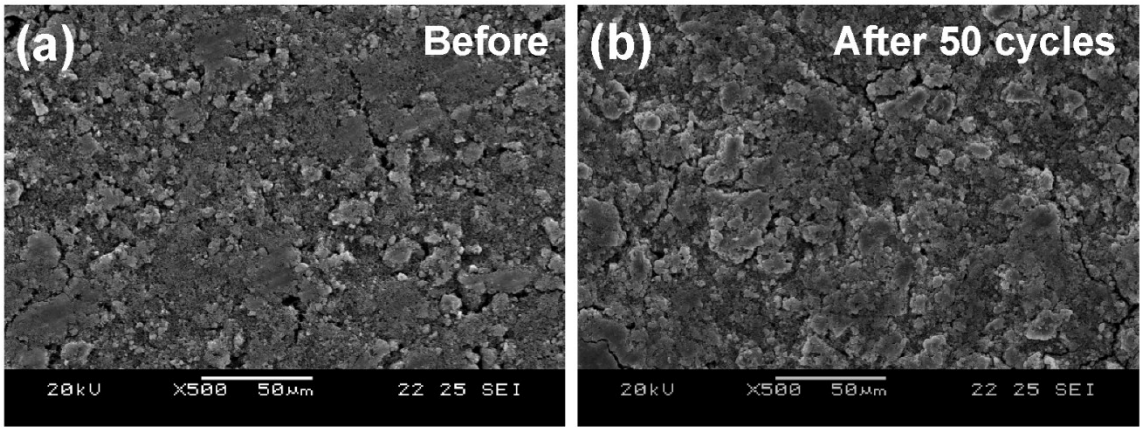

Figure S10. Changes in the electrode surface morphologies of the milled acetylene black electrodes (a) before and (b) after 50 cycles.

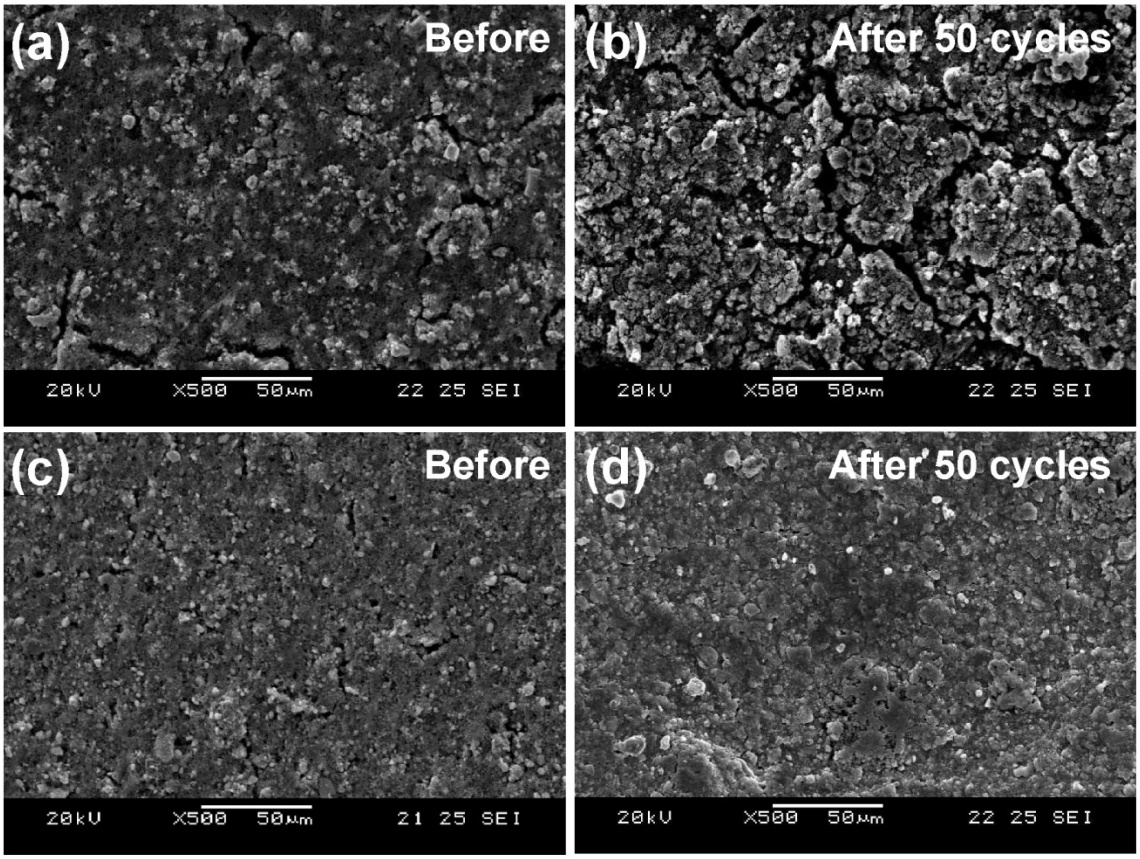

Figure S11. Changes in the electrode surface morphologies of the (a and b) pure CuP_2 and (c and d) CuP_2/C hybrid electrodes before and after 50 cycles.

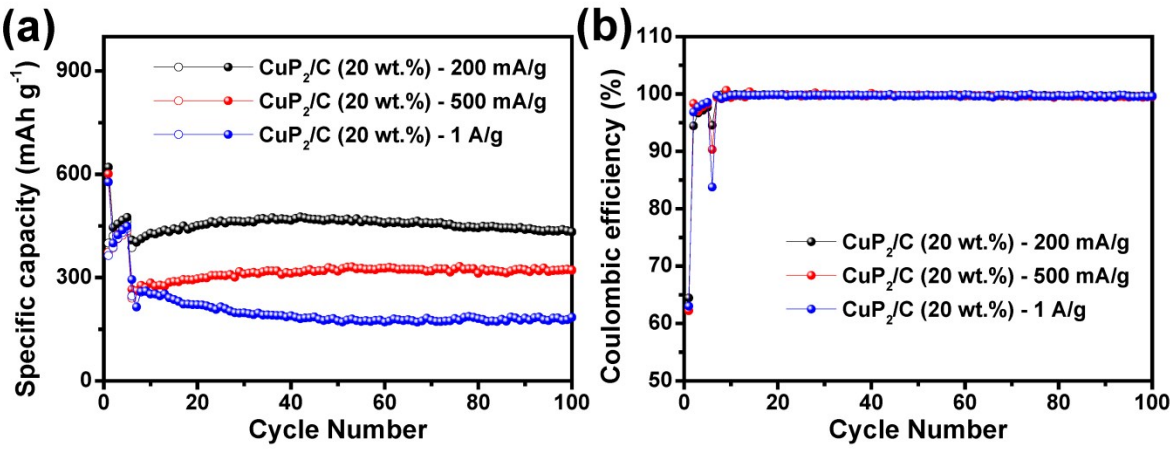

Figure S12. Comparison of the (a) cycle performance and (b) corresponding coulombic efficiency of the CuP_2/C hybrid electrodes at various current densities. The cells were tested at 50 mA g^{-1} for the initial 5 cycles for activation.